Stresses generated in cooling viscoelastic ice shells: Application to Europa

F. Nimmo
Department of Earth and Space Sciences, University of California, Los Angeles, California, USA

Received 11 August 2004; revised 22 September 2004; accepted 4 October 2004; published 3 December 2004.

[1] A cooling viscoelastic ice shell overlying an ocean develops stresses due to two effects: thermal contraction of the ice due to cooling and the expansion of the shell due to the ice-water volume change. The former effect generates near-surface compression and deeper extension; the second effect generates extension only. In both cases, stresses are smaller at depth due to viscous creep. The resulting combined stresses are extensional except at shallow (<1 km) depths in thin ice shells. For ice shells thicker than 45 km, stresses are extensional throughout. The extensional stresses exceed 10 MPa for shells thicker than 20 km and thus dominate all other likely sources of stress as long as shell cooling occurs. The dominantly extensional nature of the stresses may help to explain the puzzling lack of compression observed on Europa and other large icy satellites. However, after 100 Myr of conductive cooling the maximum theoretical elastic strains for Europa are ~0.35%, which are probably insufficient to explain the total amount of observed extension. *INDEX TERMS:* 5475 Planetology: Solid Surface Planets: Tectonics (8149); 5455 Planetology: Solid Surface Planets: Origin and evolution; 6218 Planetology: Solar System Objects: Jovian satellites; 8010 Structural Geology: Fractures and faults; 8160 Tectonophysics: Rheology—general; *KEYWORDS:* extension, tectonics

Citation: Nimmo, F. (2004), Stresses generated in cooling viscoelastic ice shells: Application to Europa, *J. Geophys. Res.*, *109*, E12001, doi:10.1029/2004JE002347.

1. Introduction

[2] The large icy satellites of Jupiter, Europa, Ganymede and Callisto, are all thought to possess oceans beneath an ice shell [*Spohn and Schubert*, 2003]. This ice shell is a few to a few tens of km thick on Europa [*Pappalardo et al.*, 1998; *Greenberg et al.*, 2000; *Schenk*, 2002], and ~100 km thick on Ganymede and Callisto [*Kivelson et al.*, 2002; *Zimmer et al.*, 2000]. The thickness of the ice shells is determined by the balance between heat production, from radiogenic elements in the silicate interior and possible tidal deformation, and conductive or convective heat loss [*Hussmann et al.*, 2002]. Radiogenic heat production decays monotonically with time; tidal heat production may fluctuate owing to feedbacks between the dissipation rate and the internal structure of the satellite [*Hussmann and Spohn*, 2004]. Thus all three Galilean satellites are likely to have experienced episodes during which the ice shell cooled and thickened with time. This paper will explore the consequences of such cooling on the deformation histories of these satellites. The key result is that near-surface, predominantly extensional stresses of several 10's of MPa will be generated as a floating ice shell thickens; the stresses are confined to a relatively shallow (few km) level because viscous relaxation reduces the stresses at greater depths, where ice viscosity is low.

0148-0227/04/2004JE002347$09.00

[3] The generation of large, extensional stresses is important for two reasons. Firstly, this mechanism may help to explain the long-standing puzzle that abundant evidence of extension, but almost none of compression, is observed on Ganymede and Europa [*Squyres and Croft*, 1986]. Secondly, the magnitude of the predicted stresses exceeds both diurnal tidal stresses and likely stresses due to nonsynchronous rotation, and thus may be a major driver of icy satellite deformation.

[4] The above issues are discussed in more detail with respect to Europa in section 5. Section 2 discusses the theory, and section 3 presents example results. Section 4 analyses the simplifications and uncertainties in the model.

2. Theory

[5] The tectonic effects of cooling spherical silicate bodies have been investigated for more than a century. In an important paper, *Darwin* [1887] showed that a cooling Earth would experience compression at the surface and extension below a depth which increases in a linear fashion with time. More recently, *Turcotte* [1983] demonstrated that extensional stresses can be generated at the surface of a cooling planet if contraction in the deep interior is small. Many studies of icy satellites have focused on the tectonic effects of differentiation [*Squyres and Croft*, 1986; *Mueller and McKinnon*, 1988; *Kirk and Stevenson*, 1987; *Cassen et al.*, 1982]. *Cassen et al.* [1979] concluded that freezing of a 100 km thick liquid layer on Europa could lead to

1% global expansion, although *Squyres* [1980] concluded that such freezing was unlikely to be an important source of stress for Ganymede or Callisto. *McKinnon* [1981] applied the consequences of expansion of a spherical cap to tectonic features on Ganymede. Both *Zuber and Parmentier* [1984] and *Hillier and Squyres* [1991] investigated the viscoelastic deformation arising from solid satellite thermal evolution; the latter paper forms the starting point for the analysis presented here.

[6] This analysis differs in two main ways from the majority of papers referred to above. Firstly, it is carried out for a spherical shell, rather than for a solid sphere, because of the subsurface oceans in the Galilean satellites. Secondly, it takes into account the large volume change which water undergoes on freezing, an effect which can generally be neglected for the analogous silicate case. On the other hand, it neglects the high pressure ice phase changes investigated by *Hillier and Squyres* [1991] and is thus appropriate to relatively thin (<150 km) ice shells.

[7] Consider an ice shell which overlies an ocean and which is cooling, and thus thickening, with time. For a purely conductive case (i.e., neglecting convection or internal heating) the shell thickness t_c and temperature structure are given by the Stefan solution [*Turcotte and Schubert*, 2002]. A shell which has thickened by an amount Δt_c will generate a radial outward motion (uplift) of the shell surface u, where

$$u = \Delta t_c \frac{\Delta\rho}{\rho} \frac{f}{1 + (f\Delta\rho/\rho)} \quad , \quad f = \left(1 - \frac{2t_c}{R_s}\right), \tag{1}$$

R_s is the satellite radius, t_c is the initial shell thickness, ρ is the density of ice and $\Delta\rho$ is the density contrast between ice and water. This outward motion will be referred to below as the volume change effect. Note that this equation reduces to the usual isostatic case [*Turcotte and Schubert*, 2002] for $t_c \ll R_s$ ($f \approx 1$).

[8] If the ice behaves as an elastic medium, then the outward motion of the shell will give rise to extensional elastic strains [*Timoshenko and Goodier*, 1970]. At the same time, because the ice is cooling, it will tend to contract (the thermal contraction effect). This contraction can lead to either compression or extension, depending on the boundary conditions. Both of these effects will be investigated below; for convenience, they will initially be treated separately, though in practice both will be occurring. In either case, the ice will behave in an elastic fashion at low temperatures, but at higher temperatures the stresses generated are likely to relax through viscous creep. Since this creep can potentially limit the maximum stresses and elastic strains generated, it is important to take viscous deformation into account.

2.1. Thermal Contraction Effect

[9] The thermal contraction effect was investigated for solid icy satellites by *Hillier and Squyres* [1991]. Their analysis applied to spheres, while here we will adapt it to ice shells. Also, these authors examined bodies which increased in temperature with time (generating predominantly extensional stresses), while here we are concerned with cooling bodies. We also adopt the sign convention of *Timoshenko and Goodier* [1970] in which extension of an individual parcel of ice is caused by an increase in temperature, and is positive (compression is negative).

[10] For a viscoelastic medium, such as ice, the stress-strain rate relation is given by

$$\frac{d\epsilon}{dt} = \frac{1}{E}\frac{d\sigma}{dt} + \frac{\sigma}{2\mu}, \tag{2}$$

where t is time, ϵ is strain, σ is stress, E is Young's modulus and μ is (temperature-dependent) viscosity [*Hillier and Squyres*, 1991]. The characteristic timescale of the system is given by the Maxwell time, μ/E; at times much shorter than this the material behaves in an elastic fashion, while over much longer timescales it behaves as a viscous medium.

[11] *Hillier and Squyres* [1991] applied this relationship and the equations of deformation in an elastic shell [*Timoshenko and Goodier*, 1970] to obtain expressions for the rate of change of stresses in the spherical icy satellite. These expressions may be adapted to a cooling ice shell by applying the bottom boundary condition to the (time-dependent) base of the ice shell, rather than the centre of the satellite. The resulting equation is as follows:

$$\begin{aligned}\frac{(1-\nu)}{2E}\frac{d\sigma_r}{dt} = &-\int_{R_i}^{r}\frac{1}{12\mu}\frac{d\sigma_r}{dr}dr + \frac{1}{r^3}\int_{R_i}^{r}\frac{d}{dt}r^2\alpha dr + \left[\frac{r^3 - R_i^3}{r^3\Phi}\right] \\ &\cdot\left[\int_{R_i}^{R_s}\frac{1}{12\mu}\frac{d\sigma_r}{dr} - \frac{1}{R_s^3}\int_{R_i}^{R_s}\frac{d}{dt}r^2\alpha dr\right].\end{aligned} \tag{3}$$

[12] Here

$$\Phi = \frac{R_s^3 - R_i^3}{R_s^3}, \tag{4}$$

ν is the Poisson's ratio, σ_r is the radial stress, r is the radial distance outward, $R_i(t)$ is the radial distance to the base of the shell and α is given by $\alpha_l \Delta T$, where α_l is the linear thermal expansivity and ΔT is the change in temperature from the initial temperature at this particular depth. The boundary conditions are zero radial stress at the top and bottom of the shell. This equation simplifies to equation (A18) of *Hillier and Squyres* [1991] for $R_i = 0$ ($\Phi = 1$), as required.

[13] Given the radial stress σ_r, the tangential stress σ_t may be obtained from

$$\sigma_t = \sigma_r + \frac{r}{2}\frac{d\sigma_r}{dr} \tag{5}$$

and the total tangential strain taken up by nonviscous deformation estimated by

$$\epsilon_t = \frac{(1-\nu)}{E}\sigma_t. \tag{6}$$

[14] If the viscosity is large, equation (3) shows that the viscous relaxation terms (which involve μ) are unimportant. In this case, the radial stress is proportional to the total temperature change and equation (3) reduces to that for the thermal stresses in a purely elastic shell (see below). The viscous terms are more important toward the base of the shell (where μ is lower) and act to reduce the radial stress.

[15] Equation (3) shows that the rate of strain increase is governed by the rate of change of temperature dT/dt. For a purely conductive ice shell which is solidifying, this rate of change is given by the Stefan solution [*Turcotte and Schubert*, 2002]

$$\frac{dT}{dt} = \frac{-(T_b - T_s)}{\mathrm{erf}\lambda_1} \exp\left(-y^2/4\kappa t\right) \frac{y}{2\left(\pi\kappa t^3\right)^{1/2}}, \tag{7}$$

where λ_1 is a constant depending on the thermal properties and latent heat of the material, y is depth below the surface and κ is thermal diffusivity. Here we are assuming a Cartesian geometry, which is appropriate for shells which are much thinner than the planetary radius. The surface and base of the ice shell are at temperatures T_s and T_b, respectively.

[16] Equation (3) allows σ_r to be calculated as a function of r and time, given the changing temperature structure of the ice shell. As noted by *Hillier and Squyres* [1991], a problem with equation (3) is that the computational time step is set by the Maxwell time, which may be very much smaller than thickening timescale for the ice shell. This problem can be reduced by assuming that all stresses below a particular isotherm T_{rel} are relaxed instantaneously. This assumption is implemented simply by defining the location of the effective base of the shell ($R_i(t)$) at a temperature T_{rel} rather than the melting temperature T_b. In practice, this modification has no effect on the results. The numerical implementation of equation (3), and the verification of this approach, is discussed further in Appendix B.

2.2. Volume Change Effect

[17] The volume change effect may be calculated using a similar approach to that of *Hillier and Squyres* [1991], but this time the top boundary condition is that the uplift $u(t)$ is specified (equation (1)). The derivation of the resulting stress is somewhat more complicated, and is given in Appendix A. The resulting rate of change of radial stress is given by

$$\begin{aligned} \frac{(1-\nu)}{2E}\frac{d\sigma_r}{dt} = &-\int_{R_i}^{r} \frac{1}{12\mu}\frac{d\sigma_r}{dr}dr + \left[\frac{r^3 - R_i^3}{r^3\Theta}\right] \\ &\cdot \left[\frac{1}{R_s}\frac{du}{dt} + \frac{\nu}{E}\left(\frac{d\sigma_r}{dt}\right)_{r=R_s} + \frac{R_s}{12}\left(\frac{1}{\mu}\frac{d\sigma_r}{dr}\right)_{r=R_s} \right. \\ &\left. + 2\int_{R_i}^{R_s} \frac{1}{12\mu}\frac{d\sigma_r}{dr}dr\right], \end{aligned} \tag{8}$$

where Θ is a constant $\approx$3. As with equation (3), there are both viscous and elastic terms. The viscous terms are not quite identical to those in equation (3) because of the differing top boundary condition. For the elastic terms, the stresses now depend on the amount of uplift u. This equation may be implemented in a similar manner to that of equation (3). One additional complication is that the term $d\sigma_r/dt$ appears on both sides of the equation; the procedure is to first solve for this term at $r = R_s$, then use this value to obtain $d\sigma_r/dt$ at other depths. Further details of the implementation are given in Appendix B.

2.3. Parameters

[18] Although the elastic parameters of ice in the laboratory are well-determined [*Gammon et al.*, 1983], the bulk properties of fractured ice shells may be rather different [*Nimmo*, 2004]. Following *Hillier and Squyres* [1991], we will adopt E = 5 GPa and ν = 0.3, and will investigate the effects of uncertainties in the former below.

Table 1. Nominal Parameters Adopted

Variable	Value	Units
T_s	100	K
T_{rel}	180	K
κ	10^{-6}	$m^2\ s^{-1}$
ν	0.3	-
ρ	1000	$kg\ m^{-3}$
Q	40	kJ/mol
C_p	2100	$J\ kg^{-1}\ K^{-1}$
T_b	270	K
R_s	1500	km
E	5	GPa
α_l	10^{-4}	K^{-1}
$\Delta\rho$	100	$kg\ m^{-3}$
μ_b	10^{15}	Pa s
g	1.3	$m\ s^{-2}$

[19] The rheology of ice is complicated, involving several different deformation mechanisms, some of which are non-Newtonian [*Goldsby and Kohlstedt*, 2001]. However, as discussed in section 4, the exact details of the ice rheology have very little effect on the final results. We will therefore assume a simplified ice rheology, with a Newtonian viscosity $\mu(T)$ that takes the form

$$\mu(T) = \mu_b \exp\left(\frac{Q(T_b - T)}{RT_bT}\right), \tag{9}$$

where T is temperature, μ_b is the reference viscosity at the base of the ice shell, temperature T_b, Q is the activation energy and R is the gas constant. Typical ice viscosities near the melting point are in the range 10^{13}–10^{15} Pa s [*Pappalardo et al.*, 1998]. We will adopt a relatively high viscosity of 10^{15} Pa s at 270 K, and show in section 4 that reasonable variations in this parameter have no effect on the near-surface stresses. The activation energy is assumed to be 40 kJ/mol, though this may be reduced if the non-Newtonian nature of ice is important [*Goldsby and Kohlstedt*, 2001]. We also assume that the effective base of the elastic ice shell is determined by T_{rel} = 180 K, and that the Stefan parameter λ_1 = 0.65. The parameters adopted are summarized in Table 1.

3. Results

[20] Figure 1 shows the results of the thermal contraction model, starting from an initial shell thickness of 2.4 km (see Appendix B). The stress profile as a function of time is shown in Figure 1a, and demonstrates that stresses are compressional at the surface, and extensional at depth. This result is similar to that obtained by *Darwin* [1887], and for a similar reason. At shallow depths, deeper layers are cooling more rapidly (equation (7)), contracting and thus putting the layers above them into compression. This effect is complicated by viscous relaxation in the warmer ice, which confines the stresses to shallower depths than expected from the purely elastic Darwin model. The tangential stresses at the surface are always compressional,

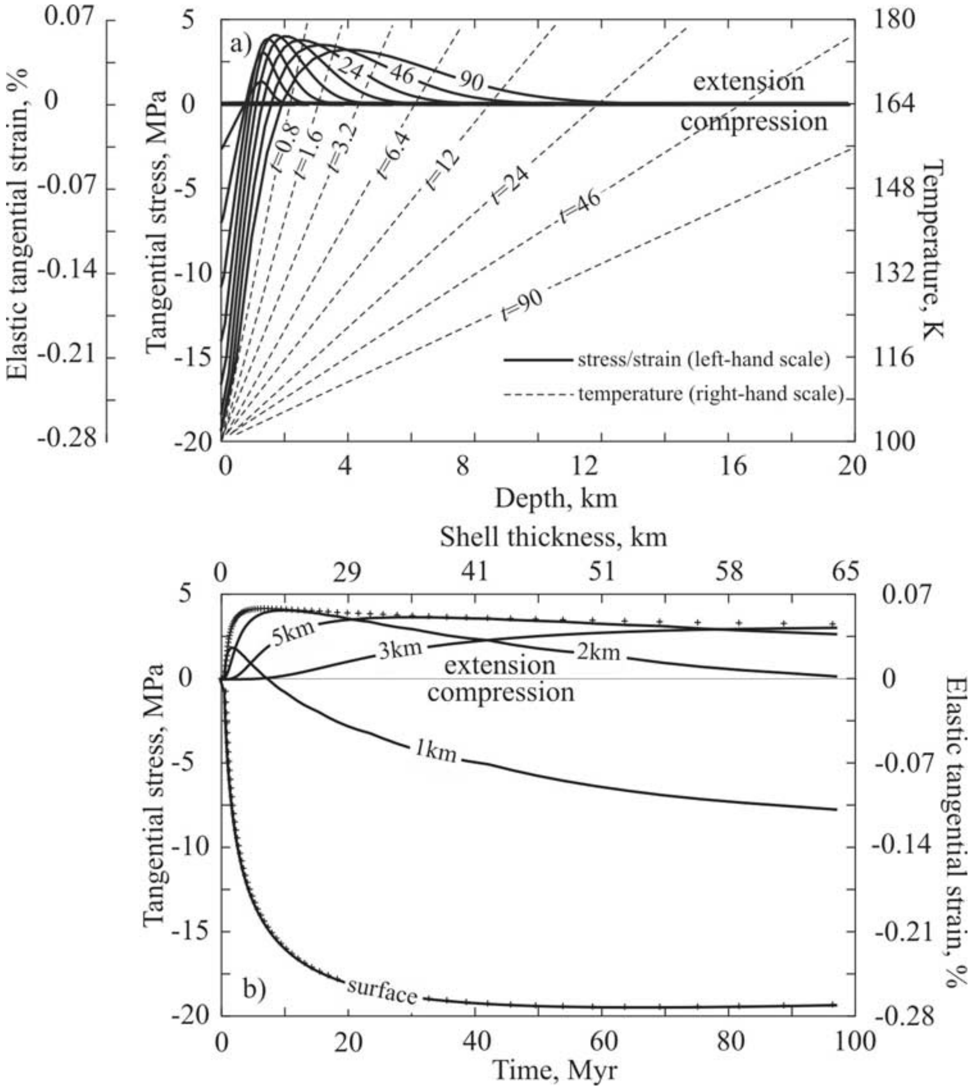

Figure 1. (a) Profiles of tangential stress against depth at different times, caused by the thermal contraction effect (equation (3)). Dashed lines are temperature (right-hand scale) calculated from Stefan solution; numbers are time (t) in Myr. Solid lines are tangential stresses, calculated at same times as for temperature profiles. Elastic strains are calculated from stresses using equation (6). The Young's modulus is 5 GPa and reference viscosity 10^{15} Pa s; other parameters given in Table 1. (b) Tangential stresses at different depths as a function of time. Crosses give the maximum and minimum values; note the changing time step as the shell thickens. Shell thickness calculated as a function of time using the Stefan solution with λ_1 = 0.65.

and the radial stresses are several orders of magnitude smaller.

[21] For a purely elastic thin shell, the maximum tangential stresses are given by [*Timoshenko and Goodier*, 1970]

$$\sigma_t = \pm \frac{E\alpha_l \Delta T_{\max}}{2(1-\nu)}, \qquad (10)$$

where $\Delta T_{\max}$ is the maximum change in temperature (this expression may also be derived from equation (3) in the limit of infinite viscosity). The surface tangential stresses shown in Figure 1a are comparable to the value of 29 MPa expected from equation (10) ($\Delta T_{\max}$ = 80 K), indicating that viscous relaxation is a relatively minor effect. Using progressively higher reference viscosities results in stresses which approach those given by equation (10).

[22] Figure 1b shows the evolution of stresses at particular depths in the ice shell with time, and the envelope of maximum and minimum stresses. As is evident from Figure 1a, at any particular depth stresses are likely to start in extension and move to compression as the shell thickens. This is the behaviour shown at 1 km depth; material at 3 km and 5 km depth has yet to experience compression. The maximum extensional stresses actually begin to decrease with time, owing to viscous relaxation in the warm ice. The maximum compressional stresses show less of such an effect because viscous relaxation is slower at cold, near-

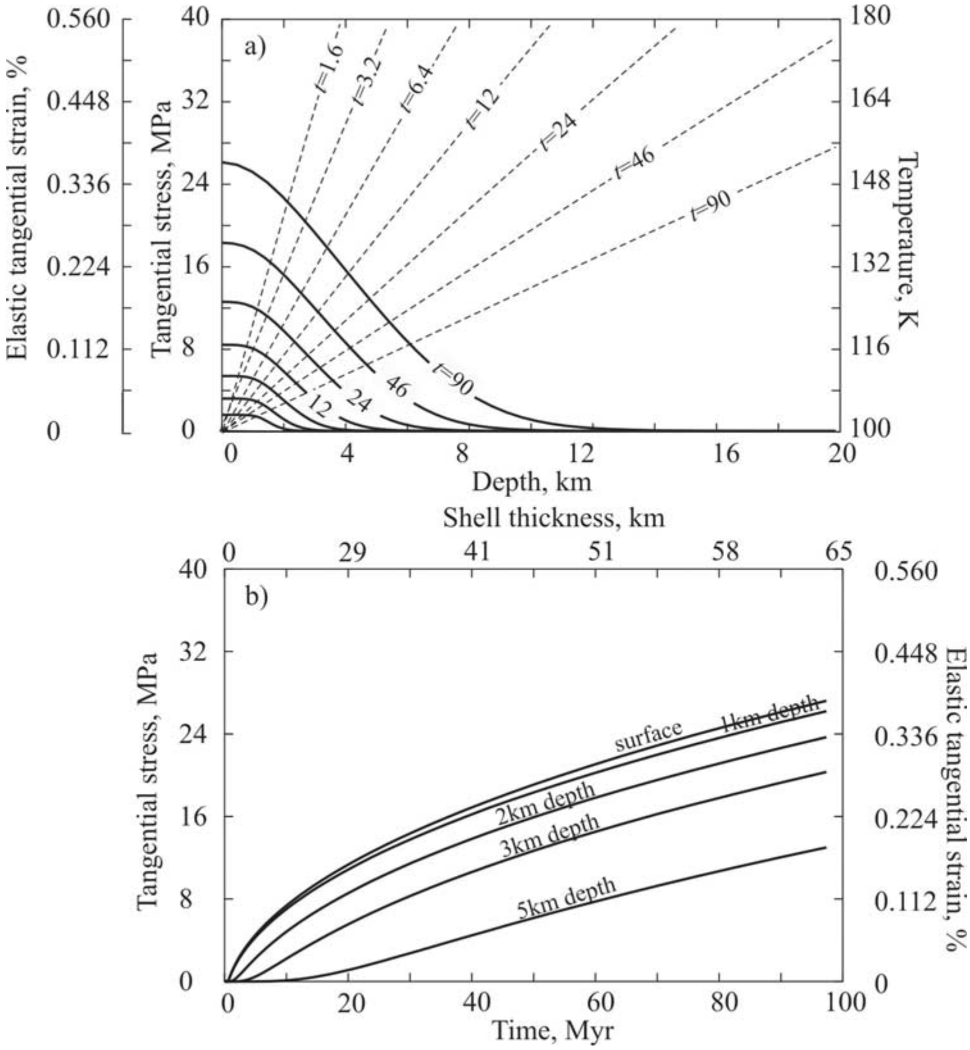

Figure 2. As for Figure 1, but calculating the stresses from the volume change effect (equation (16)).

surface temperatures. A general conclusion of this model is that, except for a thin near-surface layer, extensional stresses are likely to dominate.

[23] The magnitude of these extensional stresses is limited by viscous relaxation, and in Figure 1 they do not exceed 4 MPa. The near-surface compressional stresses are larger, because viscous relaxation is less important at colder temperatures, and approach -20 MPa. The elastic strains implied by these stresses (equation (6)) are 0.056% and -0.28%, respectively. Note that these strains are independent of the value of E assumed.

[24] Figure 2 shows the results of the volume change model. Figure 2a shows the evolution of the tangential stress profile with time. The surface tangential stress is that expected for a purely elastic shell (equation (A8)); stresses at all depths are tensional, because the outer elastic portion of the shell is moving outward. The stresses, however, decrease with increasing depth, because the warmer ice allows more viscous relaxation of the stresses. After 90 Myr, stresses have relaxed at depths exceeding about 10 km ($T \approx$ 125 K); this relaxation behaviour is identical to that seen in Figure 1a. At 125 K, the viscosity of ice is about 10^{24} Pa s and the material has a Maxwell time of ~6 Myr. Thus, after O(10) Maxwell times, the material is behaving in a predominantly viscous fashion. This result is similar to that of *Mancktelow* [1999], who found that viscoelastic materials act in a fully viscous fashion at times greater than 100 Maxwell times. For the nominal parameters, ice at the surface has a viscosity of 10^{28} Pa s and a Maxwell time of ~80 Gyr. It is therefore clear that near-surface ice is unlikely to behave in a viscous fashion for any reasonable timescales and material parameters.

[25] Figure 2b shows the evolution of stress at different depths within the ice shell from the volume change effect. As expected, the stresses are maximized at the surface, and decrease with depth (where viscous relaxation is more important). The rate of increase in surface stress with time is governed by the rate of shell thickening, which in this case is simply proportional to $t^{-1/2}$. The maximum stresses and corresponding strains after 100 Myr of cooling are comparable in magnitude to those in Figure 1b. Because the rate of increase of stress is decreasing, viscous relaxation will propagate to progressively shallower depths as time increases. However, as noted above, the effective viscosity of near-surface ice is so high that it will behave elastically essentially indefinitely.

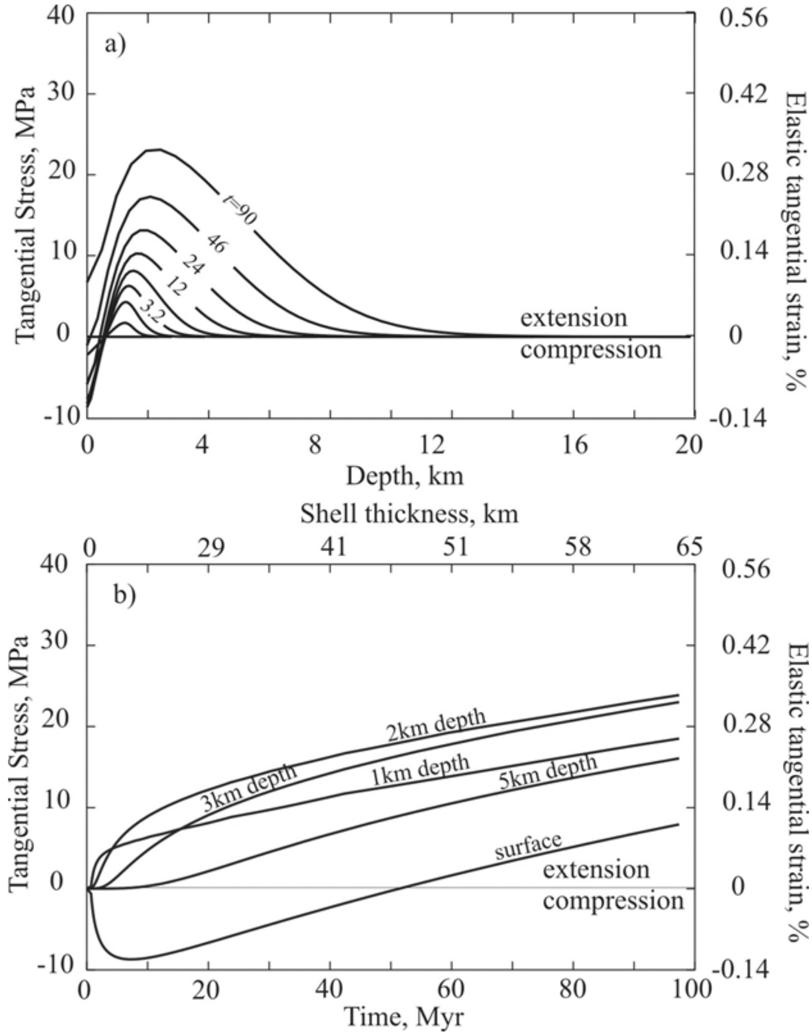

Figure 3. (a) Stress-depth profiles at different times (t) obtained by summing stresses in Figures 1a and 2a. Unlabeled profiles are at times 0.8 Myr, 1.6 Myr, and 6.4 Myr. (b) Evolution of stresses at different depths obtained by summing stresses in Figures 1b and 2b. Positive stresses are extensional. Note that entire shell is in extension after 50 Myr.

[26] Figures 1 and 2 show some similarities, in particular stress relaxation with depth. However, the resulting stress distributions are quite different. In the thermal contraction case, the surface stresses are compressional, while in the volume change case, they are extensional throughout. The time evolution of the stresses is also different. The surface tangential stresses in Figure 1 approach their maximum at early times, and do not vary much thereafter, while the surface stresses in Figure 2 increase continually.

[27] The principle of superposition allows elastic stress fields to be added [*Timoshenko and Goodier*, 1970]. No such principle exists for viscoelastic materials, but at near-surface temperatures, where the bulk of the deformation is elastic, the combined effects of thermal contraction and volume change will be closely approximated by summing the two stress contributions. Figure 3 shows the effect of carrying out this summation. Figure 3a shows that, except at early times and depths <1 km, the summed stresses are extensional and closely resemble the volume-change stress distribution (Figure 2a). Figure 3b shows how the combined stresses at different depths vary with time and demonstrates that even at depths as shallow as 1 km, the combined stresses are always extensional. At times exceeding 50 Myr (shell thickness 45 km), stresses are extensional at all depths.

[28] As a final point, it should be noted that equations (3) and (8) can equally well be applied to ice shells which are heating up and thinning. The results will be opposite to those presented here for cooling, with compression dominating except at shallow depths at early times.

4. Complications and Uncertainties

[29] Figures 1–3 neglect several likely complications in ice shell behaviour. Perhaps the most important is the fact that the temperature profile in the cooling shell may not reflect that of the simple Stefan solution. Tidal dissipation, if present in the shell, will move the isotherms closer to the surface and delay the rate of cooling. Both effects will favor viscous over elastic deformation. However, near-surface

temperatures are so cold that viscous relaxation is still likely to be minor. Thus the main effect of tidal heating is that the timescale to reach a particular shell thickness will be longer than that for the purely conductive case. However, the near-surface stress distribution characteristic of a particular shell thickness will not be strongly affected by the time it takes to reach this shell thickness, because the Maxwell time of near-surface ice is long compared to likely cooling timescales.

[30] A more serious modeling problem arises if convection initiates within the ice shell. Currently, it is not clear what minimum shell thickness is required to initiate convection; realistic, non-Newtonian ice viscosities typically imply thicker shells than Newtonian viscosities, but the uncertainties are presently large [*McKinnon*, 1999; *Nimmo and Manga*, 2002; *Showman and Han*, 2004; A. Barr et al., Convective instability in ice I with non-Newtonian rheology: Application to the icy Galilean satellites, submitted to *Journal of Geophysical Research*, 2004]. A very important consequence of convection is that the stagnant, conductive lid thickness is independent of the total shell thickness [*Solomatov*, 1995]. This conductive lid will be the only part of the shell in which elastic stresses are important, and will have a temperature structure which does not change with time (assuming constant heat production). Thus the contribution from thermal contraction stresses will be negligible. However, if the total shell is still thickening, because of an imbalance between heat production and heat transport, the volume change stresses will still apply, as in the conductive case. Thus even the onset of convection will not change the general shape of the near-surface stresses, as long as the shell continues to thicken. It is also important to note that the typical convective stresses are unlikely to exceed 0.1 MPa [*Tobie et al.*, 2003], and are thus much smaller than the stresses calculated here.

[31] The near-surface stresses of order 10 MPa calculated here are so large that the ice is likely to yield. On the basis of surface observations, this yielding most probably takes the form of brittle failure [*Zuber and Parmentier*, 1984], though plastic flow is another possibility. Brittle failure will reduce the local stresses. However, on Europa it has been observed that tectonic features commonly cross other features, such as bands, without any deflection. This suggests that healing of tectonic features is a relatively rapid process on icy satellites, and thus that the long-term accumulation of strains is unlikely to be affected by temporary yielding. Models similar to Figure 1 were carried out with the compressional stresses being reset to zero when they exceeded a critical value (to simulate brittle failure), and allowed to increase as normal thereafter. The total elastic strain was not significantly different from the case when no brittle failure was allowed.

[32] The analysis of section 2 is appropriate for an ice shell, and thus neglects processes, such as differentiation, happening within the satellite interior. Though such processes may have profound effects on satellite tectonics [*Kirk and Stevenson*, 1987; *Squyres and Croft*, 1986; *Mueller and McKinnon*, 1988], they are generally confined to the earliest history of the satellites and are unlikely to be relevant to the case of Europa (discussed below) which has a surface age <100 Myr [*Zahnle et al.*, 2003]. Similarly, this analysis neglects phase changes in ice shells, and is thus appropriate to shells thinner than 150 km or so, depending on the gravitational acceleration.

[33] One would expect that varying the ice viscosity only has a significant effect in relatively warm parts of the shell, and this turns out to be the case. For instance, reducing the reference viscosity to 10^{14} Pa s and 10^{13} Pa s allows viscous relaxation to take place at depths of 8 km and 6 km after 100 Myr. The near-surface stresses, however, are unchanged simply because of the very high near-surface ice viscosity. In a similar fashion, changing the activation energy will alter the depth at which viscous relaxation becomes important, but will have no effect on near-surface stresses.

[34] Since the elastic stresses are proportional to the Young's modulus, changing E results in a corresponding change in stress. Even for a conservatively low value for E of 1 GPa, stresses still approach 5 MPa after 100 Myr. The strain, however, remains unchanged. Changing E also changes the Maxwell time, and thus the depth at which viscous relaxation occurs, but this effect is very small.

5. Application of Results

[35] The results of section 3 may be summarized as follows: cooling ice shells will initially experience shallow (<1 km) compressional stresses and deeper extensional stresses. As time progresses, the extensional stresses will increase in magnitude and dominate at progressively shallower depths. The peak extensional stresses exceed 10 MPa for a shell thickness >20 km, while the maximum compressional stresses occur at early times and are a factor of 3 smaller. After ≈50 Myr of cooling the whole ice shell will be in extension (Figure 3). The maximum extensional stresses and strains after 100 Myr approach 25 MPa and 0.35%, respectively, while the maximum compressional values are a factor of 3 smaller. In this section we apply these model predictions to Europa.

[36] A puzzling aspect of Europa's deformation is that it is dominated by extension [e.g., *Squyres and Croft*, 1986]. Long-wavelength undulations interpreted as folds have been identified in one area [*Prockter and Pappalardo*, 2000], and some double ridges may have accommodated compression [*Patterson et al.*, 2004], but the vast majority of tectonic features are extensional. In particular, many of the features termed bands accommodate extension in a manner similar to mid-ocean ridges on Earth [*Sullivan et al.*, 1998; *Prockter et al.*, 2002] and occupy roughly 5% of the surface area in two mapped swaths [*Figueredo and Greeley*, 2004].

[37] The stresses responsible for surface deformation on Europa have been estimated at a few MPa on the basis of the requirements of fault motion down to depths of 1–3 km [*Pappalardo et al.*, 1999] and flexural bending stresses [*Nimmo et al.*, 2003a]. These stresses greatly exceed the maximum diurnal tidal stresses of ~0.1 MPa [*Greenberg et al.*, 1998; *Hoppa et al.*, 1999]; as a result, the source of the stresses responsible for the observed deformation is also somewhat puzzling. One possibility is an episode of polar wander or nonsynchronous rotation, which can generate stresses of a few MPa [*Leith and McKinnon*, 1996]. Although the spatial distribution of fractures on Europa has been used to infer various amounts of nonsynchronous rotation [*Greenberg et al.*, 2002; *Kattenhorn*, 2002; *Spaun et al.*, 2003; *Sarid et al.*, 2004], there is as yet no consensus

on whether any such rotation has actually occurred. Compositional buoyancy [*Nimmo et al.*, 2003b; *Pappalardo and Barr*, 2004] is another mechanism for providing stresses of a few MPa, but requires a thick shell and significant lateral variations in impurity content. Localized thermal stresses due to convection are unlikely to exceed 0.1 MPa [*Tobie et al.*, 2003] because the driving temperature contrast is only of order 10 K [*Nimmo and Manga*, 2002]. It is therefore clear that the ~10 MPa stresses arising from cooling are likely to dominate all other sources of stress, particularly for thick ice shells.

[38] There are four lines of evidence suggesting that the ice shell of Europa is not in steady-state (see also the discussions by *Pappalardo et al.* [1999] and *Figueredo and Greeley* [2004]). Firstly, its surface age of ≈60 Myr [*Zahnle et al.*, 2003], coupled with the fact that very few of the impact craters are tectonically deformed [*Figueredo and Greeley*, 2004], suggests that some kind of relatively rapid resurfacing event occurred. Secondly, there are wide variations in the estimates of both total shell thickness [*Pappalardo et al.*, 1998; *Greenberg et al.*, 2000; *Schenk*, 2002] and effective elastic thickness [*Billings and Kattenhorn*, 2004]. These discrepancies may partly be due to spatial variations in these quantities, but could also be due to temporal variations in shell properties. Thirdly, regional-scale geological mapping suggests that certain types of features, notably chaos terrain, occur mainly near the top of the stratigraphic column [*Figueredo and Greeley*, 2004]. While this effect might be due to difficulties in identifying ancient chaos terrains, it suggests that the geological behaviour of Europa has changed with time. Finally, Europa's orbital and thermal evolution are intimately coupled, and recent models suggest that significant changes in tidal dissipation, and thus shell thickness, can occur on timescales comparable to the estimated surface age [*Hussmann and Spohn*, 2004].

[39] If Europa's ice shell has indeed thickened over time, the results of Figures 1–3 may help to explain observations of its geological behaviour. Firstly, the magnitude of the stresses implied (a few tens of MPa) can easily account for stresses inferred from the tectonic features (see above). Secondly, the preponderance of extensional features becomes easy to understand. As argued above, although shallow (<1 km) stresses will initially be compressional, as the shell thickens extensional stresses will increasingly dominate (Figure 3a). Thus preexisting compressional features are likely to be overprinted by later extensional features. The absence of observed compressional features suggests that the volume change stresses are dominant, and thus that the shell is relatively thick (Figure 3). Figure 3 also suggests that peak extensional stresses are likely to occur at depths of 1–2 km, broadly compatible with geologically inferred brittle-ductile transition depths [*Pappalardo et al.*, 1999].

[40] Although the predicted stress magnitudes and predominantly extensional style agree well with observations, the predicted strains are more problematic. Figure 3 shows that the extensional elastic strains after 100 Myr cooling do not exceed 0.35%. Conversely, the extension accommodated by bands is closer to 5% [*Figueredo and Greeley*, 2004]. This order of magnitude difference cannot be explained by any of the uncertainties discussed above: the maximum elastic strains are of order $\alpha_l \Delta T$ and u/R_s for the thermal contraction and volume change models, respectively, and cannot generate 5% strains for reasonable temperature structures and shell thicknesses. We are left with two possibilities: either there are additional processes at work, such as yielding, which generate increased extensional strains in response to the stresses; or compressional features must be common on the surface of Europa, but have not yet (in most cases) been identified.

6. Summary and Conclusions

[41] Stresses will be generated in a thickening ice shell due to two effects: contraction from cooling, and extension due to the volume change of freezing water. The combined stresses will be extensional, except at shallow (<1 km) depths and for low shell thicknesses. The magnitude of these stresses exceeds 10 MPa for shells in excess of 20 km thickness, and probably exceeds any other likely source of stress. The dominance of extensional stresses may help to explain the lack of observed compressional features on the surface of Europa. However, the elastic strains implied by this model are an order of magnitude smaller than inferred amounts of surface extension. Either the predicted stresses result in more extension than expected for a purely elastic medium (e.g., due to yielding), or there are as yet unidentified locations of compression on Europa.

Appendix A

[42] Here the stresses caused by the volume change effect (see section 2) are derived. In a spherical elastic shell, we have [*Timoshenko and Goodier*, 1970]

$$\frac{d\sigma_t}{dt} = \frac{d\sigma_r}{dt} + \frac{r}{2}\frac{d}{dt}\frac{d\sigma_r}{dr} \tag{A1}$$

and also

$$\frac{d\sigma_t}{dt} = \frac{E}{r(1-\nu)}\frac{du'}{dt} + \frac{\nu}{1-\nu}\frac{d\sigma_r}{dt}, \tag{A2}$$

where u' is the (radial) displacement at r and the tangential strain is given by u'/r.

[43] From *Hillier and Squyres* [1991, equation (A17)] we have, neglecting effects due to cooling and correcting their final plus sign to a minus,

$$\frac{1-\nu}{2E}\frac{d\sigma_r}{dt} = \frac{C_1}{3} + \frac{C_2}{r^3} - \int_{R_i}^{r} \frac{1}{12\mu}\frac{d\sigma_r}{dr}dr, \tag{A3}$$

where C_1 and C_2 are constants to be determined by the boundary conditions. The first boundary condition, $\sigma_r = 0$ at $r = R_i$, is straightforward and yields

$$C_1 = -3\frac{C_2}{R_i^3}. \tag{A4}$$

[44] The second boundary condition is a specified displacement $u(t)$ at $r = R_s$. To apply this boundary condition, we first calculate the surface tangential stresses by differ-

entiating equation (A3), substituting into equation (A1) and applying equation (A2):

$$\frac{(1-\nu)}{E}\frac{d\sigma_t}{dt} = \frac{2C_1}{3} - \frac{C_2}{r^3} - 2\int_{R_i}^{r}\frac{1}{12\mu}\frac{d\sigma_r}{dr}dr - \frac{r}{12\mu}\frac{d\sigma_r}{dr}$$
$$= \frac{1}{r}\frac{du'}{dt} + \frac{\nu}{E}\frac{d\sigma_r}{dt}. \quad \text{(A5)}$$

Applying the boundary condition that $u' = u(t)$ at $r = R_s$ and making use of equations (A3) and (A4), we finally obtain

$$\frac{(1-\nu)}{2E}\frac{d\sigma_r}{dt} = -\int_{R_i}^{r}\frac{1}{12\mu}\frac{d\sigma_r}{dr}dr + \left[\frac{r^3 - R_i^3}{r^3\Theta}\right]\left[\frac{1}{R_s}\frac{du}{dt} + \frac{\nu}{E}\left(\frac{d\sigma_r}{dt}\right)_{r=R_s} + \frac{R_s}{12}\left(\frac{1}{\mu}\frac{d\sigma_r}{dr}\right)_{r=R_s} + 2\int_{R_i}^{R_s}\frac{1}{12\mu}\frac{d\sigma_r}{dr}dr\right], \quad \text{(A6)}$$

where

$$\Theta = 2 + \left(\frac{R_i}{R_s}\right)^3. \quad \text{(A7)}$$

[45] Equation (A6) is the equivalent of equation (A18) of *Hillier and Squyres* [1991], in that it allows the evolution of σ_r as a function of depth and time to be calculated, given the specified evolution of the surface uplift $u(t)$. The first two terms inside the large bracket are the elastic response; the other terms are due to the finite viscosity. It can be seen by inspection that $d\sigma_r/dt = 0$ at $r = R_i$.

[46] If the viscosity is very large, the terms involving μ may be neglected and equation (A6) may then be simplified. After some algebra, it yields

$$\sigma_r\,|_{r=R_s} = \frac{2Eu\epsilon}{(1-\nu)R_s}, \quad \sigma_t\,|_{r=R_s} = \frac{Eu}{(1-\nu)R_s}\left(1 + \frac{2\epsilon\nu}{1-\nu}\right), \quad \text{(A8)}$$

where $\epsilon = (R_s/R_i) - 1$.

Appendix B

[47] Here the numerical implementation of equations (3) and (8) is described. An explicit, finite-difference approach was used, with a constant grid spacing in the relevant part of the ice shell. 61 vertical grid points were used, with the grid spacing updated each time step to take into account the growing ice shell. This updating necessitated interpolation of the stresses onto the new grid spacing each time step. The base temperature T_{rel} was set to 180 K; stresses at greater depths were assumed to relax instantaneously.

[48] The initial temperature conditions were obtained by solving the Stefan problem for a shell of thickness 2.4 km. Temperatures were recalculated at time steps given by $0.1\Delta z^2/\kappa$, where Δz is the grid spacing; this time step was not allowed to exceed 1000 yrs. For each point, stresses were updated using equations (3) or (8) at time steps of $0.5\mu/E$ or 0.1 times the temperature time step, whichever was smaller. The nature of equations (3) and (8) mean that a runaway occurs if $\sigma_r < 0$. To avoid this occurring, if the change in σ_r in any time step would have resulted in $\sigma_r < 0$, σ_r was set to zero.

[49] Increasing T_{rel} to 200 K from 180 K resulted in no detectable change in the final stress distribution in Figure 2. This was to be expected, since ice at such high temperatures relaxes stresses in a viscous fashion. Reducing the number of grid points from 61 to 31 resulted in the stresses shown in Figure 2 changing by <0.1%. By setting the reference viscosity to a high value (10^{35} Pa s), it was verified that the elastic stresses (equations (10) and (A8)) were recovered.

[50] **Acknowledgments.** I am grateful to Bob Pappalardo for helpful discussions, and Walter Kiefer and an anonymous reviewer for constructive suggestions. Funded by NASA PGG grant NNG04GE89G.

References

Billings, S. E., and S. A. Kattenhorn (2004), The great thickness debate: Ice shell thickness models for Europa and comparisons with estimates based on flexure at ridges, *Icarus*, in press.

Cassen, P., R. T. Reynolds, and S. J. Peale (1979), Is there liquid water on Europa?, *Geophys. Res. Lett.*, *6*, 731–734.

Cassen, P. M., S. J. Peale, and R. T. Reynolds (1982), Structure and thermal evolution of the Galilean satellites, in *Satellites of Jupiter*, edited by D. Morrison, pp. 93–128, Univ. of Ariz. Press.

Darwin, G. H. (1887), Note on Mr. Davison's paper on the straining of the Earth's crust in cooling, *Philos. Trans. R. Soc. London, Ser. A*, *178*, 242–249.

Figueredo, P., and R. Greeley (2004), Resurfacing history of Europa from pole-to-pole geological mapping, *Icarus*, *167*, 287–312.

Gammon, P. H., H. Kiefte, M. J. Clouter, and W. W. Denner (1983), Elastic constants of artificial and natural ice samples by Brillouin spectroscopy, *J. Glaciol.*, *29*, 433–460.

Goldsby, D. L., and D. L. Kohlstedt (2001), Superplastic deformation of ice: Experimental observations, *J. Geophys. Res.*, *106*, 11,017–11,030.

Greenberg, R., et al. (1998), Tectonic processes on Europa: Tidal stresses, mechanical response and visible features, *Icarus*, *135*, 64–78.

Greenberg, R., P. Geissler, B. R. Tufts, and G. V. Hoppa (2000), Habitability of Europa's crust: The role of tidal-tectonic processes, *J. Geophys. Res.*, *105*, 17,551–17,562.

Greenberg, R., G. V. Hoppa, P. Geissler, A. Sarid, and B. R. Tufts (2002), The rotation of Europa, *Celest. Mech. Dyn. Astron.*, *83*, 35–47.

Hillier, J., and S. W. Squyres (1991), Thermal stress tectonics on the satellites of Saturn and Uranus, *J. Geophys. Res.*, *96*, 15,665–15,674.

Hoppa, G. V., B. R. Tufts, R. Greenberg, and P. E. Geissler (1999), Formation of cycloidal features on Europa, *Science*, *285*, 1899–1902.

Hussmann, H., and T. Spohn (2004), Europa's ice shell thickness derived from thermal-orbital evolution models, in *Europa's Icy Shell*, *LPI Contrib. 1195*, 7012, Lunar and Planet. Inst., Houston, Tex.

Hussmann, H., T. Spohn, and K. Wieczerkowski (2002), Thermal equilibrium states of Europa's ice shell: Implications for internal ocean thickness and surface heat flow, *Icarus*, *156*, 143–151.

Kattenhorn, S. A. (2002), Nonsynchronous rotation evidence and fracture history in the Bright Plains region, Europa, *Icarus*, *157*, 490–506.

Kirk, R., and D. Stevenson (1987), Thermal evolution of a differentiated Ganymede and implications for surface features, *Icarus*, *69*, 91–134.

Kivelson, M. G., K. K. Khurana, and M. Volwerk (2002), The permanent and inductive magnetic moments of Ganymede, *Icarus*, *157*, 507–522.

Leith, A. C., and W. B. McKinnon (1996), Is there evidence for polar wander on Europa?, *Icarus*, *120*, 387–398.

Mancktelow, N. S. (1999), Finite-element modelling of single-layer folding in elasto-viscous materials: The effect of initial perturbation geometry, *J. Struct. Geol.*, *21*, 161–177.

McKinnon, W. B. (1981), Tectonic deformation of Galileo Regio and limits to the planetary expansion of Ganymede, *Lunar Planet. Sci.*, *12B*, 1585–1597.

McKinnon, W. B. (1999), Convective instability in Europa's floating ice shell, *Geophys. Res. Lett.*, *26*, 951–954.

Mueller, S., and W. B. McKinnon (1988), Three-layered models of Ganymede and Callisto: Compositions, structures and aspects of evolution, *Icarus*, *76*, 437–464.

Nimmo, F. (2004), What is the Young's modulus of ice?, in *Europa's Icy Shell*, *LPI Contrib. 1195*, 7005, Lunar and Planet. Inst., Houston, Tex.

Nimmo, F., and M. Manga (2002), Causes, characteristics and consequences of convective diapirism on Europa, *Geophys. Res. Lett.*, *29*, 2109, doi:10.1029/2002GL015754.

Nimmo, F., B. Giese, and R. T. Pappalardo (2003a), Estimates of Europa's ice shell thickness from elastically supported topography, *Geophys. Res. Lett.*, *30*, 1233, doi:10.1029/2002GL016660.

Nimmo, F., R. T. Pappalardo, and B. Giese (2003b), On the origins of band topography, *Europa, Icarus*, *166*, 21–32.

Pappalardo, R. T., and A. C. Barr (2004), The origin of domes on Europa: The role of thermally induced compositional diapirism, *Geophys. Res. Lett.*, *31*, L01701, doi:10.1029/2003GL019202.

Pappalardo, R. T., et al. (1998), Geological evidence for solid-state convection in Europa's ice shell, *Nature*, *391*, 365–368.

Pappalardo, R. T., et al. (1999), Does Europa have a subsurface ocean? Evaluation of the geological evidence, *J. Geophys. Res.*, *104*, 24,015–24,055.

Patterson, G. W., J. W. Head, and R. T. Pappalardo (2004), Convergent boundaries on Europa: A numerical approach to Euler pole analysis and its implications for plate reconstruction, *Lunar Planet Sci.*, *XXXV*, 1590.

Prockter, L. M., and R. T. Pappalardo (2000), Folds on Europa: Implications for crustal cycling and accommodation of extension, *Science*, *289*, 941–943.

Prockter, L. M., J. W. Head III, R. T. Pappalardo, R. J. Sullivan, A. E. Clifton, B. Giese, R. Wagner, and G. Neukum (2002), Morphology of Europan bands at high resolution: A mid-ocean ridge-type rift mechanism, *J. Geophys. Res.*, *107*(E5), 5028, doi:10.1029/2000JE001458.

Sarid, A. R., R. Greenberg, G. V. Hoppa, P. Geissler, and B. Preblich (2004), Crack azimuths on Europa: Time sequence in the southern leading face, *Icarus*, *168*, 144–157.

Schenk, P. (2002), Thickness constraints on the icy shells of the Galilean satellites from a comparison of crater shapes, *Nature*, *417*, 419–421.

Showman, A. P., and L. Han (2004), Numerical simulations of convection in Europa's ice shell: Implications for surface features, *J. Geophys. Res.*, *109*, E01010, doi:10.1029/2003JE002103.

Solomatov, V. S. (1995), Scaling of temperature-dependent and stress-dependent viscosity convection, *Phys. Fluids*, *7*, 266–274.

Spaun, N. A., R. T. Pappalardo, and J. W. Head (2003), Evidence for shear failure in forming near-equatorial lineae on Europa, *J. Geophys. Res.*, *108*(E6), 5060, doi:10.1029/2001JE001499.

Spohn, T., and G. Schubert (2003), Oceans in the icy Galilean satellites of Jupiter?, *Icarus*, *161*, 456–467.

Squyres, S. W. (1980), Volume changes in Ganymede and Callisto and the origin of grooved terrain, *Geophys. Res. Lett.*, *7*, 593–596.

Squyres, S. W., and S. K. Croft (1986), The tectonics of icy satellites, in *Satellites*, edited by J. A. Burns and M. S. Matthews, pp. 293–341, Univ. of Ariz. Press, Tucson.

Sullivan, R., et al. (1998), Episodic plate separation and fracture infill on the surface of Europa, *Nature*, *391*, 371–372.

Timoshenko, S. P., and J. N. Goodier (1970), *Theory of Elasticity*, 3rd ed., McGraw-Hill, New York.

Tobie, G., G. Choblet, and C. Sotin (2003), Tidally heated convection: Constraints on Europa's ice shell thickness, *J. Geophys. Res.*, *108*(E11), 5124, doi:10.1029/2003JE002099.

Turcotte, D. L. (1983), Thermal stresses in planetary elastic lithospheres, *Proc. Lunar Planet. Sci. Conf. 13th*, Part 2, *J. Geophys. Res.*, *88*, suppl., A585–A587.

Turcotte, D. L., and G. Schubert (2002), *Geodynamics*, Cambridge Univ. Press, New York.

Zahnle, K., P. M. Schenk, H. F. Levison, and L. Dones (2003), Cratering rates in the outer solar system, *Icarus*, *163*, 263–289.

Zimmer, C., K. K. Khurana, and M. G. Kivelson (2000), Subsurface oceans on Europa and Callisto: Constraints from Galileo magnetometer observations, *Icarus*, *147*, 329–347.

Zuber, M. T., and E. M. Parmentier (1984), Lithospheric stresses due to radiogenic heating of an ice-silicate planetary body: Implications for Ganymede's tectonic evolution, *Proc. Lunar Planet Sci. Conf. 14th*, Part 2, *J. Geophys. Res.*, suppl., *89*, B429–B437.

F. Nimmo, Department of Earth and Space Sciences, University of California, Los Angeles, CA 90095-1567, USA. (nimmo@ess.ucla.edu)